

1 **Advanced understanding of prokaryotic biofilm formation using a cost-effective and**
2 **versatile multi-panel adhesion (mPAD) mount**

3

4 Stefan Schulze^{1†}, Heather Schiller^{1†}, Jordan Solomonic², Orkan Telhan², Kyle Costa³, and
5 Mechthild Pohlschroder^{1*}

6

7 ¹Department of Biology, University of Pennsylvania, Philadelphia, PA 19104, USA

8 ²Weitzman School of Design, University of Pennsylvania, Philadelphia, PA 19104, USA

9 ³Department of Plant and Microbial Biology, University of Minnesota, St. Paul, MN 55108,
10 USA

11 [†]These authors contributed equally.

12 *Correspondence should be addressed to: Mechthild Pohlschroder, pohlschr@sas.upenn.edu

13

14 **Running head: Versatile surface adhesion mount**

15

16 **Abstract**

17

18 Most microorganisms exist in biofilms, which comprise aggregates of cells surrounded by an
19 extracellular matrix that provides protection from external stresses. Based on the conditions
20 under which they form, biofilm structures vary in significant ways. For instance, biofilms that
21 develop when microbes are incubated under static conditions differ from those formed when
22 microbes encounter the shear forces of a flowing liquid. Moreover, biofilms develop dynamically
23 over time. Here, we describe a cost-effective, 3D-printed coverslip holder that facilitates surface
24 adhesion assays under a broad range of standing and shaking culture conditions. This multi-panel
25 adhesion (mPAD) mount further allows cultures to be sampled at multiple time points, ensuring
26 consistency and comparability between samples and enabling analyses of the dynamics of
27 biofilm formation. As a proof of principle, using the mPAD mount for shaking, oxic cultures, we
28 confirm previous flow chamber experiments showing that *Pseudomonas aeruginosa* wild type
29 and a phenazine deletion mutant (Δphz) form similar biofilms. Extending this analysis to anoxic
30 conditions, we reveal that microcolony and biofilm formation can only be observed under
31 shaking conditions and are decreased in the Δphz mutant compared to wild-type cultures,
32 indicating that phenazines are crucial for the formation of biofilms if oxygen as an electron
33 acceptor is not available. Furthermore, while the model archaeon *Haloferax volcanii* does not
34 require archaella for attachment to surfaces under static conditions, we demonstrate that *H.*
35 *volcanii* mutants that lack archaella are negatively affected in their early stages of biofilm
36 formation under shaking conditions.

37 **Importance:** Due to the versatility of the mPAD mount, we anticipate that it will aid the
38 analysis of biofilm formation in a broad range of bacteria and archaea. Thereby, it contributes to
39 answering critical biological questions about the regulatory and structural components of biofilm
40 formation and understanding this process in a wide array of environmental, biotechnological,
41 and medical contexts.

42 **Key words:** *Pseudomonas aeruginosa*, bacteria, *Haloferax volcanii*, archaea, surface
43 attachment, microcolony formation, biofilms, biofilm assay, shear forces

44

45

46 **Introduction**

47 Planktonic prokaryotic cells often encounter highly stressful environmental conditions such as
48 those created by toxins or nutrient depletion. One strategy that bacteria and archaea have
49 evolved to mitigate such stress is the establishment of a biofilm: a complex microbial
50 community bound by a matrix of extracellular polymeric substances. The first steps in biofilm
51 formation are cell adherence to an abiotic surface quickly followed by cell aggregation and
52 microcolony formation; later, a mature biofilm is established. Adhesion often requires surface
53 filaments (1–3). For example, *Pseudomonas aeruginosa*, a bacterium in which biofilm formation
54 has been thoroughly studied, requires flagella and type IV pili to complete the initial steps of
55 establishing a biofilm (4). For some organisms, additional components are also involved in
56 biofilm maturation, such as redox-active secondary metabolites called phenazines. In *P.*
57 *aeruginosa*, phenazines drive the release of extracellular DNA into the biofilm matrix and
58 facilitate survival of cells in the anoxic core of a biofilm (5, 6).

59 The large variety of platforms that have been developed to study biofilm formation seemingly
60 reflects the diversity of attachment mechanisms and biofilm architectures that have evolved.
61 While evolutionarily conserved type IV pili are required for surface adhesion in many organisms
62 (7), as analyzed e.g. through simple atmosphere-liquid interface (ALI) assays in standing
63 cultures, the use of specific pilins can vary depending on the environmental conditions (2, 8, 9).
64 Furthermore, while bacterial flagella and their archaeal counterparts (archaella) facilitate the
65 binding to surfaces in some species (10), surface attachment in other species like the model
66 haloarchaeon *Haloferax volcanii* appears to be independent of archaella (11). However, the
67 involvement of type IV pili, archaella, and other cell surface structures in attachment and biofilm
68 formation may depend on the environmental conditions under which ALI assays are performed.
69 In fact, it has been shown that shear forces impact the ability of microbes to form biofilms, the
70 characteristics of the established biofilms, and the rate of detachment in prokaryotic biofilms,
71 e.g. for *Escherichia coli* (12). Therefore, it is critical to analyze the formation of biofilms under
72 various conditions, and more advanced platforms, such as complex flow chambers or rotating
73 annular bioreactors, have been used for this task (13).

74 Despite the importance of generating data that will lead to critical discoveries about the
75 molecular mechanisms that regulate the establishment of biofilms, each biofilm analysis method
76 has intrinsic limitations. For instance, the standard ALI assay cannot be used to evaluate biofilm
77 formation under flow (14) and thus prevents insight into the effect of shear forces on biofilm
78 formation. Furthermore, this type of standing assay often allows undesirable liquid biofilm
79 formation (15–17), making comparisons of planktonic and sessile cells unfeasible. As an
80 alternative, some simple assays like the BioFilm Ring Test may be performed under shaking
81 conditions, but this advantage comes with the drawback that microscopy cannot be used to
82 analyze the biofilm (14). In contrast, more complex systems like flow chambers allow for
83 detailed continuous imaging of biofilms (13, 18); however, it is extremely difficult to retrieve
84 samples for molecular biological or biochemical evaluation at various time points. Some of these
85 systems, including flow chambers and rotating annular bioreactors, are also costly (13). These
86 limitations highlight that most biofilm analysis methods face a tradeoff between high throughput
87 and detail of analysis. High-throughput platforms like the standard ALI assay or BioFilm Ring
88 Test only allow for rather superficial analyses of biofilm formation, while detailed analyses, e.g.
89 in flow chambers, suffer from comparatively low throughput and limited versatility.

90 To overcome some of these challenges, we present a detailed description of the use of an
91 inexpensive **multi-panel adhesion** (mPAD) mount for the characterization of biofilm formation.
92 This mount, which can be produced using a standard 3D printer, facilitates the analysis of cell
93 adhesion to coverslips for both standing and shaking cultures and under a variety of conditions.
94 Using the mPAD mount, the same culture can be sampled at multiple time points for
95 microscopic, biochemical, and molecular biological analyses.

96 As a proof of principle, we have analyzed *P. aeruginosa* biofilm formation under standing and
97 shaking conditions, showing not only differences in biofilm architecture and the ability to
98 proceed past the single-cell adhesion stage under anoxic conditions but also a decrease in
99 microcolony formation in a Δphz mutant strain under shaking, anoxic conditions in contrast to
100 wild-type cultures. Similarly, *H. volcanii* biofilms that formed in shaking cultures look very
101 different from biofilms established in standing cultures, and we show that the $\Delta arlA1/2$ strain
102 exhibits a decreased initial surface adhesion in shaking cultures despite lacking any defects
103 under standing conditions, highlighting the importance of testing biofilm formation in wild-type

104 and mutant strains under a variety of conditions.

105

106 **Materials and Methods**

107 *Strains and growth conditions*

108 *P. aeruginosa* PA14 and the *P. aeruginosa* Δ phz mutant (19) were grown at 37 °C in lysogeny
109 broth (orbital shaker at 250 rpm). For anaerobic growth, 40 mM sodium nitrate and 200 mM
110 MOPS were included in the medium, and cultures were grown standing inside of a heated (37
111 °C) Coy-type anoxic chamber with an atmosphere of 2-3% H₂, 10% CO₂, and balance N₂.
112 MOPS buffer was included to avoid pH changes from reduction of nitrate and the high CO₂
113 atmosphere in the chamber. For growth as a biofilm, overnight cultures were sub-inoculated,
114 grown for several hours to an OD_{600nm} between 1.0 and 1.5, and then further diluted to an OD₆₀₀
115 of 0.3. These cultures were immediately transferred to biofilm growth conditions and incubated
116 either standing in 12-well plates or shaking in Petri dishes (100 mm x 15 mm) with the mPAD
117 mount (see below).

118

119 *H. volcanii* H53 as well as the *H. volcanii* Δ arlA1/2 mutant were grown at 45 °C in liquid
120 (orbital shaker at 250 rpm) or on solid agar (containing 1.5% (wt/vol) agar) semi-defined
121 casamino acid (Hv-Cab) medium (20), supplemented with tryptophan (+Trp) and uracil (+Ura) at
122 a final concentration of 50 µg ml⁻¹. A colony from a solid Hv-Cab plate (incubated for three to
123 five days at 45 °C) was inoculated into 5 mL Hv-Cab liquid medium. After incubating the
124 culture tubes overnight at 45 °C with shaking (orbital shaker at 250 rpm) until the strains reached
125 mid-log phase (OD_{600nm} ~0.7) the strains were diluted to an OD_{600nm} of 0.01 into a final volume
126 of 20 mL followed by incubation at 45 °C with shaking (orbital shaker at 250 rpm) until cultures
127 reached an OD_{600nm} of 0.35. Each culture was then transferred into either a 12-well plate or a
128 sterile plastic Petri dish (100 mm x 15 mm) for biofilm growth conditions (see below).

129

130 *Printing of mPAD mount*

131 The 3D model of the mPAD mount can be downloaded from Thingiverse
132 (<https://www.thingiverse.com/thing:4784964>). A Form 2 (Formlabs) 3D printer using a High

133 Temp resin (Formlabs) was used to print mPAD mounts that can be sterilized in an autoclave.
134 These mounts were used for the *P. aeruginosa* biofilm assays. Conversely, an MP Mini Delta 3D
135 printer (Monoprice) using polylactic acid (PLA) filament (Monoprice) was employed to 3D-print
136 the mPAD mounts used for assays with *H. volcanii*.

137

138 *Setting up the mPAD mount for adhesion assays under standing and shaking conditions*

139 *P. aeruginosa* biofilms: glass coverslips (22 mm x 22 mm x 1.5 mm, Fisher Scientific) were
140 marked to be able to distinguish the two sides (facing inward and outward from the mPAD) as
141 well as the top and bottom of the coverslip. When inserting the coverslips into the mPAD mount,
142 thin pieces of aluminum foil were placed at the top of the coverslip to enable a tighter fit.
143 Assembled mPADs were autoclaved to sterilize all surfaces. *P. aeruginosa* culture (grown and
144 diluted as described above) was placed in the bottom half of a Petri dish, and the mPAD mount
145 was placed on top of the Petri dish with each coverslip reaching at least 0.5 cm into the culture.
146 The Petri dish lid was placed on top of the mPAD mount before incubating the assembled setup
147 in a humidified chamber at 37 °C. Cell attachment was allowed to occur for 30 minutes before
148 placing the chamber on an orbital shaker set to 60 rpm. For static biofilms, 2 ml of culture at
149 OD_{600nm} 0.3 was aliquoted into a 12-well plate (Falcon) with a glass coverslip placed into each
150 well. Both wild-type and Δphz biofilms were grown via the methods described above under both
151 oxic and anoxic conditions.

152 *H. volcanii* biofilms: mPAD mounts were washed with 70% ethanol and allowed to air dry
153 before inserting the marked coverslips (see above) into the slits of the mPAD mount. Thin pieces
154 of autoclaved aluminum foil were placed at the top of the coverslip to enable a tighter fit in the
155 mPAD mount. The mPAD mount with inserted coverslips was placed onto the bottom half of the
156 Petri dish containing the liquid culture with each coverslip reaching at least 0.5 cm into the
157 culture. The Petri dish lid was placed on top of the mPAD mount before placing the Petri dish
158 with the mPAD mount into a humidified chamber. The cultures were incubated at 45 °C on an
159 orbital shaker set to 60 rpm. For static biofilms, 2 ml of *H. volcanii* culture at OD_{600nm} 0.35 was
160 aliquoted into a 12-well plate (Falcon) with a glass coverslip placed into each well. Both wild-
161 type and $\Delta arlA1/2$ biofilms were grown via the methods described above under oxic conditions.

162

163 *Staining and imaging*

164 *P. aeruginosa* biofilms: coverslips were removed at 1, 6, 20, and 45 hours, submerged briefly in
165 0.5% NaCl to wash off loosely attached cells, and fixed by placing the coverslip in 3 ml of a
166 0.5% NaCl/2% glutaraldehyde solution in a 12-well plate for 30 minutes at room temperature.
167 For anaerobically grown cultures, the fixation step was performed inside the anoxic chamber
168 before moving coverslips into an oxic atmosphere for further processing. After fixation, the
169 coverslips were immediately placed into 3 ml of 0.1% crystal violet for 10 minutes. After
170 staining, coverslips were washed in H₂O and allowed to dry before imaging. Coverslips were
171 imaged on an ECHO Revolve R4 hybrid microscope with a universal slide mount. The
172 microscope was operated in the upright orientation with an extra-long working distance
173 condenser (NA 0.30, working distance 73 mm). Images were taken with either a 20x fluorite
174 (NA 0.45, working distance 6.6-7.8 mm) or 40x fluorite (NA 0.75, working distance 0.51 mm)
175 objective lens. Images were collected from the middle of the slide near the location of the ALI.

176

177 *H. volcanii* biofilms: coverslips were removed at 24 and 120 hours, submerged briefly in 18%
178 saltwater, and fixed by placing them in 2% acetic acid in small Petri dishes (Corning) for 30
179 minutes at room temperature. After fixation, the coverslips were allowed to air dry. Cells
180 attached to coverslips were stained by submerging them into 0.1% crystal violet for 10 minutes.
181 After removing the coverslips from the crystal violet solution, they were rinsed twice with H₂O
182 and air dried. Biofilms were imaged using a Leica DMi8 inverted microscope with brightfield
183 settings using 20x and 40x magnifications. Representative images of all areas of the biofilm on
184 the coverslip were taken. Images were collected from the middle of the slide near the location of
185 the ALI.

186

187

188 **Results and Discussion**

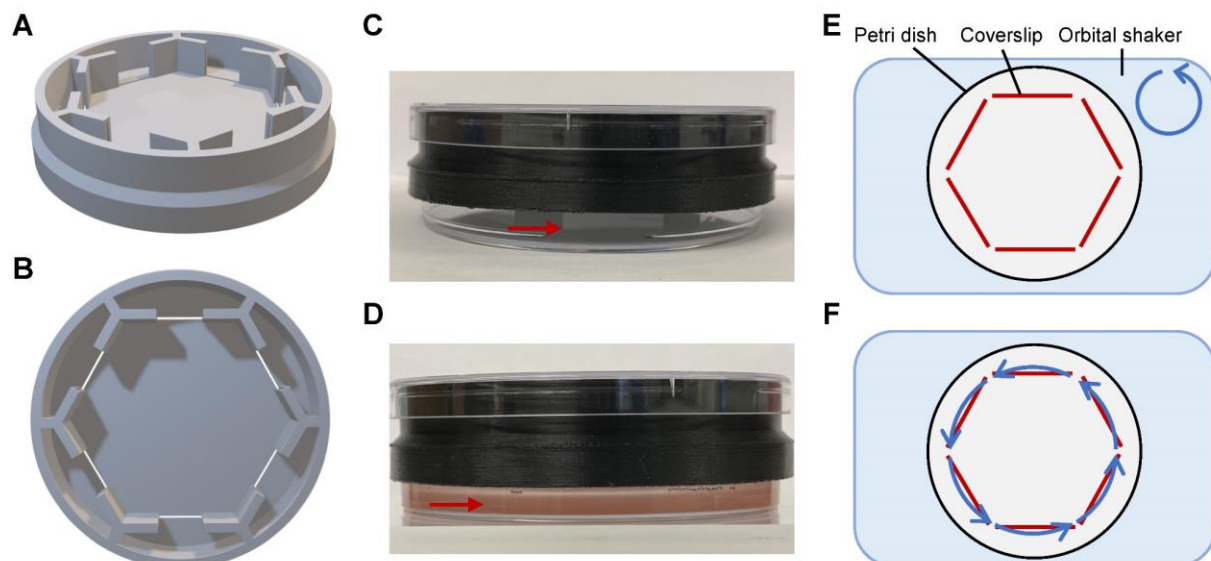
189

190 *The mPAD mount is designed as a versatile and affordable device to characterize biofilm
191 formation.*

192 Many invaluable tools have been developed over the past decades to characterize biofilm
193 formation, ranging from simple ALI assays on coverslips in 12-well plates to sophisticated flow

194 chambers that allow live observation of the stages of biofilm formation and comparison of
195 various shear forces. To combine advantages of different types of assays, we designed the mPAD
196 mount (Fig. 1). 3D-printing of the mPAD mount results in low-costs, similar to simple 12-well
197 plate assays, and its design for standard Petri dishes ensures its adaptability to different
198 environmental conditions, including shear forces generated by constant shaking on an orbital
199 shaker and an O₂-deprived atmosphere in an anaerobic chamber. Additionally, multiple slots
200 within each mPAD mount enable the observation of different stages of biofilm formation by
201 removing individual coverslips at different time points. This design also allows harvesting of
202 samples for transcriptomics or proteomics analyses from different stages of biofilm formation
203 from a single culture, thereby reducing high variabilities that can arise from the use of multiple
204 cultures. Furthermore, when used under shaking conditions, the formation of liquid biofilms,
205 which can obstruct comparative system-wide analyses because of varying planktonic
206 subpopulations, is prevented.

207



208

209 **Figure 1: The 3D-printed mPAD mount can be used for biofilm assays under a broad range**
210 **of conditions, including shaking.** A 3D-model of the mPAD mount is shown from the side (A)
211 and top (B). Coverslips can be inserted into the six slots of the mPAD mount and subsequently
212 placed onto a Petri dish (C). After filling the Petri dish with a cell culture (*H. volcanii* shown
213 here), coverslips reach into the culture (D), allowing cells to adhere to the coverslip surface. The
214 mPAD mount can be placed on an orbital shaker to expose cells to shear forces (E). The radial
215 positioning of the slots of the mPAD mount ensures that cells adhering to any coverslip
216 experience the same shear forces (F). Red arrows point to the lower end of inserted coverslips;

217 blue arrows indicate shaking of the orbital shaker and the shear forces experienced by the
218 coverslips.
219

220 Radial positioning of the six slots of the mPAD mount ensures that all coverslips are exposed to
221 the same shear force when placed on an orbital shaker (Fig. 1E-F). With this design only
222 minimal differences between the inner and outer side of the coverslip were observed (data not
223 shown). However, due to the 3D-printing of the mount, changes to the design are straight-
224 forward, and a variety of different layouts are conceivable, e.g. to increase the adhesion surface
225 area or to accommodate movement of the liquid via a stirring bar instead of an orbital shaker
226 (Supplemental Figure 1).

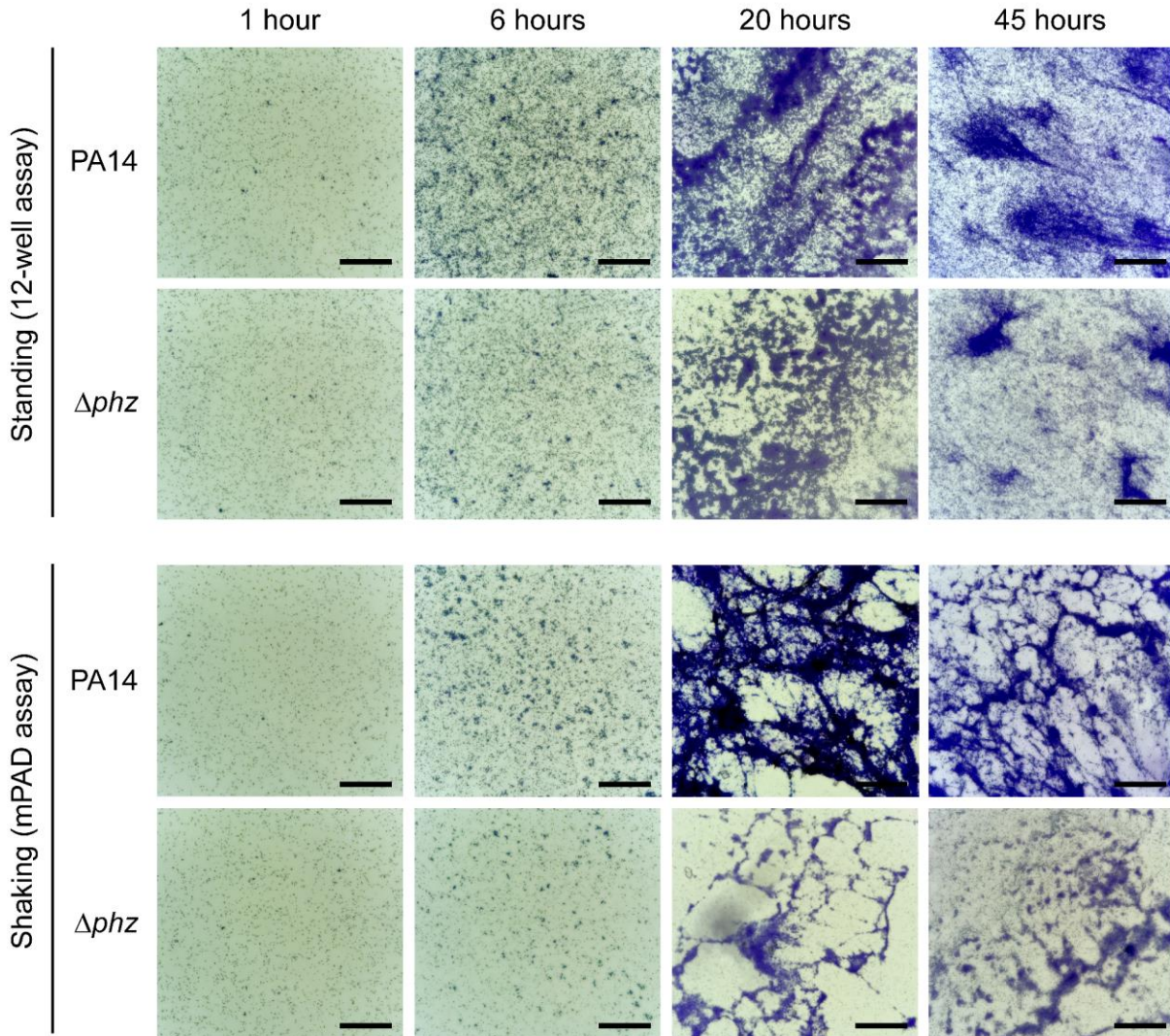
227 3D-printing of the mPAD furthermore supports a wide variety of materials, including materials
228 that show high resistance to chemicals and temperature. In this study, we have used a Form 2
229 (Formlabs) 3D printer employing a High Temp resin (Formlabs) for the *P. aeruginosa* studies, as
230 that material allows the mPAD mounts to be sterilized in an autoclave. For the biofilm studies of
231 the archaeon *H. volcanii*, an MP Mini Delta 3D printer (Monoprice) using polylactic acid (PLA)
232 filament (Monoprice) was employed to 3D-print the mPAD mount. While PLA is not as resistant
233 to heat and chemicals as Formlabs' High Temp resin, it is more affordable, and contamination of
234 *H. volcanii* mid-log phase cultures grown in media containing ~2.5 M salt are very unlikely, thus
235 semi-sterile 70% ethanol washes could be employed instead of autoclaving.

236

237 *The mPAD mount is suitable for characterization of *P. aeruginosa* wild-type and Δphz biofilms*
238 *exposed to shear forces.*

239 The use of flow chambers has established that cell exposure to shear forces plays a significant
240 role in the structure and architecture of *P. aeruginosa* biofilms (21). Similarly, employing the
241 mPAD mount setup on an orbital shaker facilitated the visualization of shear force effects on *P.*
242 *aeruginosa* cultures, because cells adhering to coverslips within this setup are experiencing shear
243 forces from the moving liquid. For wild-type *P. aeruginosa* cultures, adhesion of individual cells
244 to the coverslip after an hour was similar under shaking conditions as under standing conditions
245 using a common 12-well-plate ALI assay (Fig. 2). At six hours, microcolonies were observed,
246 and by 20 hours, mature biofilms had formed under both conditions, but the biofilms formed
247 under standing conditions were distributed more uniformly in a mixture of single cells,

248 microcolonies, and large, three-dimensional biofilm structures. In contrast, under shaking
249 conditions, cells formed large, dense, web-like structures with fewer visible unconnected
250 microcolonies and single cells. The Δphz strain showed a similar trend, although adhesion,
251 microcolony formation, and mature biofilms were overall less dense compared to the wild type.
252
253



254
255 **Figure 2: Using the mPAD mount for the analysis of *P. aeruginosa* biofilms under aerobic,**
256 **shaking conditions confirmed that exposure to shear forces leads to different biofilm**
257 **architectures and noticeable phenotype in Δphz mutant.** *P. aeruginosa* wild-type (PA14) and
258 Δphz cultures were incubated under aerobic standing and shaking conditions for 1, 6, 20, and 45
259 hours before staining adherent cells with crystal violet. Images are representative of two
260 biological replicates. Scale bar is 100 μ m.
261

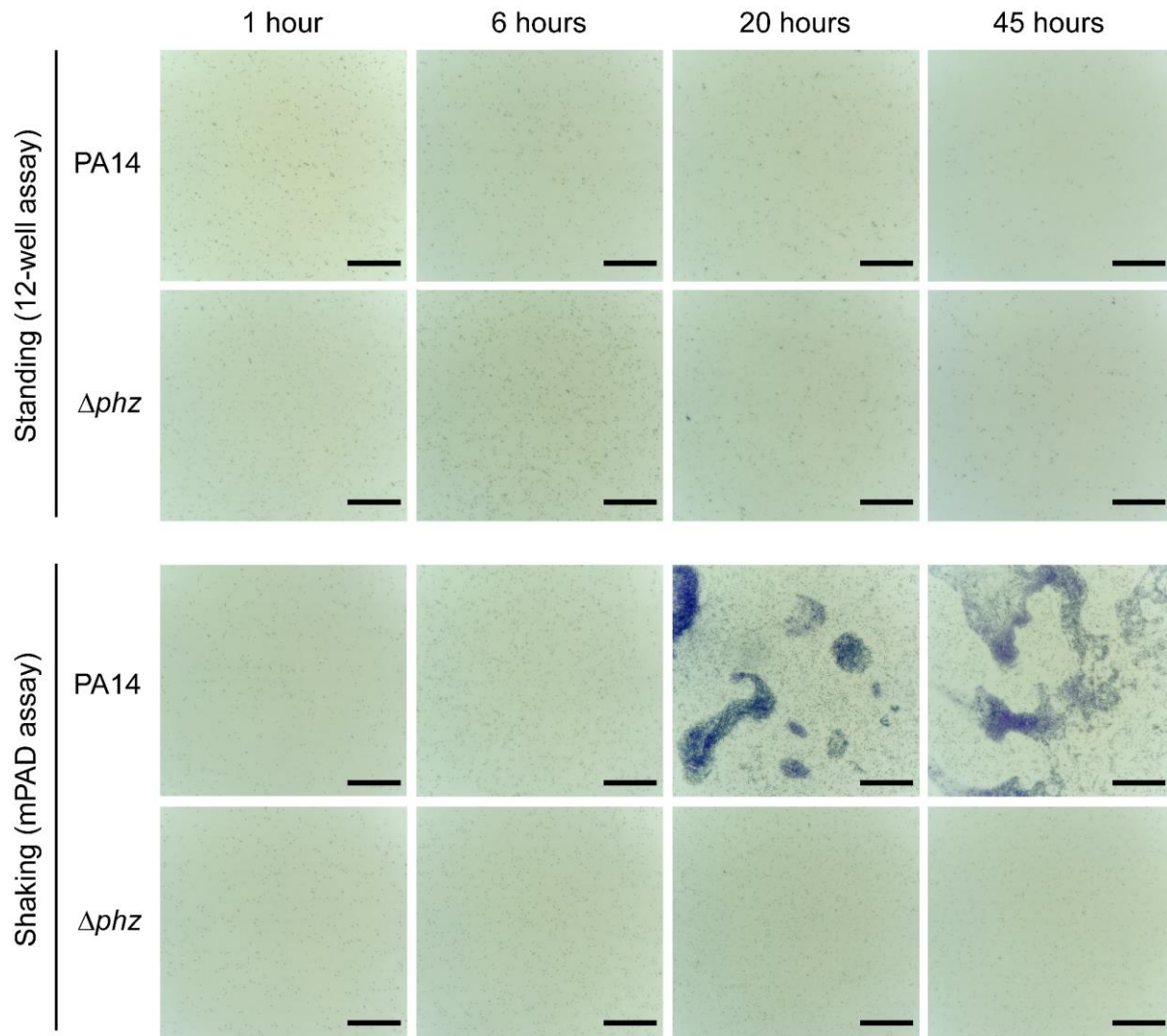
262 The results show that the mPAD mount is suitable for the analysis of different stages of biofilm
263 formation under shaking conditions, with differences in biofilm architecture that are in line with
264 previous experiments using flow chambers (6). For further analyses, cells can be washed off the
265 coverslips, e.g. to quantify adhesion through OD_{600nm} measurements of crystal violet. Untreated
266 adhering cells can also be retrieved, e.g. for -omics experiments. Thereby, the mPAD mount sets
267 the stage to compare the proteomes of biofilms formed under standing and shaking conditions to
268 determine whether the differences are mainly structural or also include changes in the
269 composition of the biofilm, including differentially expressed and post-translationally modified
270 proteins or differences in the exopolymeric substances.

271

272 *Under anaerobic conditions, P. aeruginosa only forms microcolonies when exposed to shear
273 forces.*

274 *P. aeruginosa* wild-type cultures can grow anaerobically, but comparisons of biofilm formation
275 with and without the exposure to shear forces have thus far not been reported. In addition to
276 characterizing wild-type biofilm formation under anaerobic, standing conditions, the versatility
277 of the mPAD mount facilitated the analysis of shear force impacts on surface attachment,
278 microcolony formation, and biofilm formation under anaerobic conditions. Interestingly, while
279 initial attachment to the coverslip occurred both with and without shaking, only cells exposed to
280 shear forces through orbital shaking in the mPAD assay were able to form microcolonies and
281 biofilms without available O₂, although these biofilms were significantly less dense than those
282 under aerobic conditions (Fig. 3). Similar to the wild type, the Δphz mutant was unable to form
283 microcolonies under anaerobic, standing conditions. However, in comparison to the wild type,
284 the adhesion and microcolony formation after 20 and 45 hours under anaerobic conditions were
285 reduced for Δphz and even lacking completely in one of the replicates. While this phenotype is
286 similar to the reduced biofilm formation under aerobic conditions, the more pronounced effect
287 under anaerobic conditions indicates a crucial role of *phz* as an electron acceptor when O₂ is not
288 available. This role is in line with results on electron shuttling via phenazines in *P. aeruginosa*
289 biofilms on agar plates (22).

290

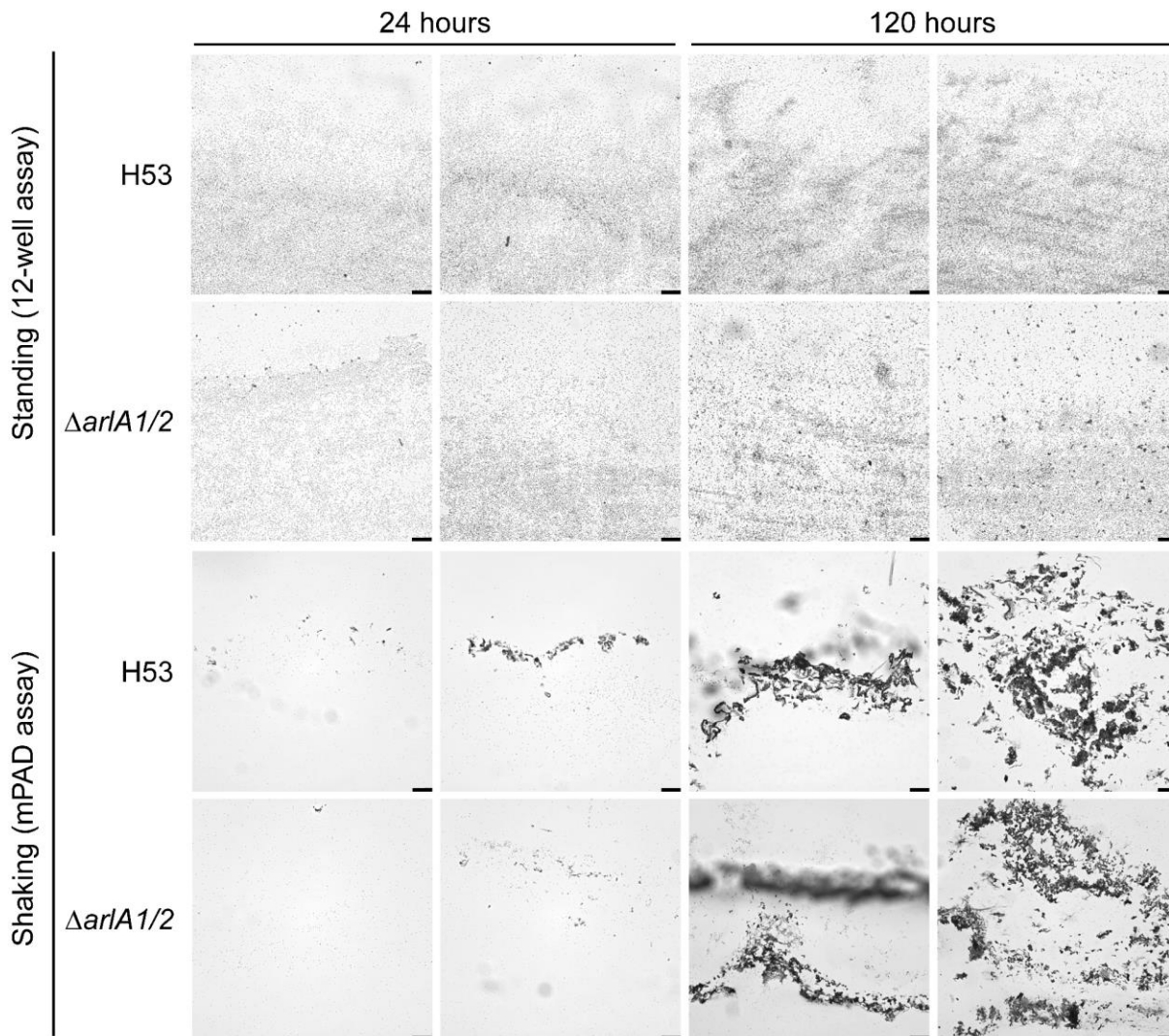


291
292 **Figure 3: Employing the mPAD under anoxic conditions revealed that shear forces**
293 **contribute to the formation of biofilms, which are dependent on *phz* under these conditions.**
294 *P. aeruginosa* wild-type (PA14) and Δphz cultures were incubated in an anaerobic chamber
295 under standing and shaking conditions for 1, 6, 20, and 45 hours before staining adherent cells
296 with crystal violet. Images are representative of two biological replicates. Scale bar is 100 μ m.
297

298 Haloferax volcanii *archaellins* contribute to effective initial adhesion when exposed to shear
299 forces.

300 While the haloarchaeon *H. volcanii* has been used as a model organism to study biofilm
301 formation in archaea (15, 16, 23), to our knowledge, biofilm assays have not been performed
302 under shaking conditions for any archaeon so far. Using the mPAD assay under shaking
303 conditions, we could show that, similar to *P. aeruginosa*, *H. volcanii* can form biofilms under

304 shaking conditions but exhibits distinct biofilm architectures depending on the exposure to shear
305 forces (Fig. 4). Under standing conditions, after 24 hours, attachment of *H. volcanii* to the
306 coverslip surface resulted in a dense layer of cells interspersed with areas of small microcolonies,
307 which developed into larger areas of dense biofilms within 120 hours. In contrast, under shaking
308 conditions, *H. volcanii* attached only sparsely as single cells to the coverslip within 24 hours, and
309 microcolonies formed as dense clusters of cells with network-like connections that likely consist
310 of extracellular substances. After 120 hours, these microcolonies grew into dense biofilm
311 structures that were connected over larger areas.
312 The process of cell adhesion and microcolony formation without exposure to shear forces is
313 independent of archaella in *H. volcanii*, as shown by the wild type-like adhesion of a $\Delta arlA1/2$
314 mutant, which lacks both archaellins (11). This observation is in contrast to many bacteria and
315 archaea for which flagella and archaella, respectively, have been shown to be required for
316 adhesion to surfaces (1, 24–27). To determine whether *H. volcanii* archaellins are required for
317 biofilm formation when cells are exposed to shear forces, we compared the attachment of *H.*
318 *volcanii* wild-type and $\Delta arlA1/2$ cultures to coverslips under shaking conditions using the mPAD
319 mount. At 120 hours, both strains were able to form microcolonies and mature biofilm structures
320 of similar magnitude and density (Fig. 4). However, at earlier stages, the mutant $\Delta arlA1/2$ strain
321 did not adhere to the same extent as the wild type. While wild-type cultures at 24 hours already
322 formed microcolonies in addition to single cell adhesion, $\Delta arlA1/2$ exhibited mainly single cell
323 adhesion, and only few, small clusters of cells were present.



324
325 **Figure 4: *H. volcanii* biofilm formation under shaking conditions differs substantially from**
326 **standing conditions and is negatively affected by a lack of archaella.** *H. volcanii* wild-type
327 (H53) and $\Delta arlA1/2$ cultures were incubated under standing and shaking conditions at 45 °C for 24
328 and 120 hours before staining adherent cells with crystal violet. Images are representative of two
329 biological replicates. Scale bar is 50 μ m.
330

331
332 These results indicate that archaella in *H. volcanii* could be involved in the initial surface
333 attachment under shaking conditions. Possible explanations for a contribution of archaella in the
334 binding to surfaces could be an increased sensing of the surface or movement toward it.
335 In general, in contrast to bacteria, the effects of shear forces on archaeal surface attachment and
336 biofilm formation have not been analyzed so far. Our initial results here suggest that valuable
337 insights into the molecular mechanisms of this process in archaea could be gained. The mPAD

338 mount provides an ideal foundation for further studies because it can be used in a broad range of
339 extreme conditions in which many model archaea thrive.

340

341

342 **Conclusion**

343

344 Biofilms represent the major life form of prokaryotes on Earth (28), and the conditions under
345 which they occur are highly diverse and often not static. Therefore, we developed the simple,
346 3D-printed, versatile and affordable mPAD mount, which can be used to study prokaryotic
347 biofilm formation under a broad variety of environmental conditions. The design of the mPAD
348 thereby allows for samples to be taken from the same culture at multiple time points for
349 microscopy as well as -omics analyses, capturing dynamic changes within the process of biofilm
350 formation.

351 We could show the usefulness of the mPAD on the examples of *P. aeruginosa* and *H. volcanii*
352 biofilm formation. For *P. aeruginosa*, we revealed that while biofilms do not form in the absence
353 of O₂ under standing conditions, they can be observed when cells are exposed to shear forces via
354 shaking of the culture. Furthermore, *P. aeruginosa* Δphz mutants are inhibited in their ability to
355 form biofilms under anaerobic, shaking conditions. For *H. volcanii*, we could show for the first
356 time that biofilms can form under shaking conditions and exhibit a different biofilm architecture
357 than under standing conditions. Additionally, *H. volcanii* archaella seem to be involved in the
358 initial surface adhesion under shaking, but not under standing, conditions. These results show not
359 only the biological insights that can be gained from biofilm assays under a variety of conditions
360 but also highlight the versatility of the mPAD mount. With the increased availability of 3D-
361 printing capabilities and the straightforward changes to the design of the mPAD, the range of
362 applications will widen even further.

363

364

365 **Acknowledgements**

366

367 We would like to thank the University of Pennsylvania Libraries' Biotech Commons for courtesy
368 3D-printing of mPAD mounts. S.S., H.S., and M.P acknowledge support from the National

369 Science Foundation Grant 1817518. K.C. acknowledges support from a Young Investigator
370 Award from the Army Research Office, grant number W911NF-19-1-0024.

371

372 **Conflict of interest**

373

374 The authors declare no conflict of interest.

375

376

377 **Bibliography**

378

- 379 1. van Wolferen M, Orell A, Albers S-V. 2018. Archaeal biofilm formation. *Nat Rev Microbiol*
380 16:699–713.
- 381 2. Pohlschroder M, Esquivel RN. 2015. Archaeal type IV pili and their involvement in biofilm
382 formation. *Front Microbiol* 06.
- 383 3. Chaudhury P, Quax TEF, Albers S-V. 2018. Versatile cell surface structures of archaea: Cell
384 surface structures of archaea. *Mol Microbiol* 107:298–311.
- 385 4. O'Toole GA, Kolter R. 1998. Flagellar and twitching motility are necessary for
386 *Pseudomonas aeruginosa* biofilm development. *Mol Microbiol* 30:295–304.
- 387 5. Glasser NR, Kern SE, Newman DK. 2014. Phenazine redox cycling enhances anaerobic
388 survival in *Pseudomonas aeruginosa* by facilitating generation of ATP and a proton-motive
389 force: Phenazines facilitate energy generation. *Mol Microbiol* 92:399–412.
- 390 6. Ramos I, Dietrich LEP, Price-Whelan A, Newman DK. 2010. Phenazines affect biofilm
391 formation by *Pseudomonas aeruginosa* in similar ways at various scales. *Res Microbiol*
392 161:187–191.
- 393 7. Berry J-L, Pelicic V. 2015. Exceptionally widespread nanomachines composed of type IV
394 pilins: the prokaryotic Swiss Army knives. *FEMS Microbiol Rev* 39:134–154.
- 395 8. Legerme G, Pohlschroder M. 2019. Limited Cross-Complementation Between *Haloferax*
396 *volcanii* PilB1-C1 and PilB3-C3 Paralogs. *Front Microbiol* 10:700.
- 397 9. Hsiao A, Toscano K, Zhu J. 2007. Post-transcriptional cross-talk between pro- and anti-
398 colonization pili biosynthesis systems in *Vibrio cholerae*: Pili biosynthesis systems in *Vibrio*
399 *cholerae*. *Mol Microbiol* 67:849–860.

400 10. Jarrell K, Ding Y, Nair D, Siu S. 2013. Surface Appendages of Archaea: Structure, Function,
401 Genetics and Assembly. *Life* 3:86–117.

402 11. Tripepi M, Imam S, Pohlschröder M. 2010. *Haloferax volcanii* Flagella Are Required for
403 Motility but Are Not Involved in PibD-Dependent Surface Adhesion. *J Bacteriol* 192:3093–
404 3102.

405 12. Fink R, Oder M, Rangus D, Raspor P, Bohinc K. 2015. Microbial adhesion capacity.
406 Influence of shear and temperature stress. *Int J Environ Health Res* 25:656–669.

407 13. Azeredo J, Azevedo NF, Briandet R, Cerca N, Coenye T, Costa AR, Desvaux M, Di
408 Bonaventura G, Hébraud M, Jaglic Z, Kačániová M, Knøchel S, Lourenço A, Mergulhão F,
409 Meyer RL, Nychas G, Simões M, Tresse O, Sternberg C. 2017. Critical review on biofilm
410 methods. *Crit Rev Microbiol* 43:313–351.

411 14. Magana M, Sereti C, Ioannidis A, Mitchell CA, Ball AR, Magiorkinis E, Chatzipanagiotou
412 S, Hamblin MR, Hadjifrangiskou M, Tegos GP. 2018. Options and Limitations in Clinical
413 Investigation of Bacterial Biofilms. *Clin Microbiol Rev* 31:e00084-16, /cmr/31/3/e00084-
414 16.atom.

415 15. Chimileski S, Franklin MJ, Papke RT. 2014. Biofilms formed by the archaeon *Haloferax*
416 *volcanii* exhibit cellular differentiation and social motility, and facilitate horizontal gene
417 transfer. *BMC Biol* 12:65.

418 16. Schiller H, Schulze S, Mutan Z, de Vaulx C, Runcie C, Schwartz J, Rados T, Bisson Filho
419 AW, Pohlschroder M. 2020. *Haloferax volcanii* Immersed Liquid Biofilms Develop
420 Independently of Known Biofilm Machineries and Exhibit Rapid Honeycomb Pattern
421 Formation. *mSphere* 5:mSphere.00976-20, e00976-20.

422 17. Armitano J, Méjean V, Jourlin-Castelli C. 2014. Gram-negative bacteria can also form
423 pellicles: Floating biofilm in Gram-negative bacteria. *Environ Microbiol Rep* 6:534–544.

424 18. Blanco-Cabra N, López-Martínez MJ, Arévalo-Jaimes BV, Martin-Gómez MT, Samitier J,
425 Torrents E. 2021. A new BiofilmChip device for testing biofilm formation and antibiotic
426 susceptibility. *Npj Biofilms Microbiomes* 7:62.

427 19. Dietrich LEP, Price-Whelan A, Petersen A, Whiteley M, Newman DK. 2006. The phenazine
428 pyocyanin is a terminal signalling factor in the quorum sensing network of *Pseudomonas*
429 *aeruginosa*. *Mol Microbiol* 61:1308–1321.

430 20. de Silva RT, Abdul-Halim MF, Pittrich DA, Brown HJ, Pohlschroder M, Duggin IG. 2021.

431 Improved growth and morphological plasticity of *Haloferax volcanii*. *Microbiology*
432 <https://doi.org/10.1099/mic.0.001012>.

433 21. Mordue J, O'Boyle N, Gadegaard N, Roe AJ. 2021. The force awakens: The dark side of
434 mechanosensing in bacterial pathogens. *Cell Signal* 78:109867.

435 22. Schiessl KT, Hu F, Jo J, Nazia SZ, Wang B, Price-Whelan A, Min W, Dietrich LEP. 2019.
436 Phenazine production promotes antibiotic tolerance and metabolic heterogeneity in
437 *Pseudomonas aeruginosa* biofilms. *Nat Commun* 10:762.

438 23. Esquivel RN, Schulze S, Xu R, Hippler M, Pohlschroder M. 2016. Identification of
439 *Haloferax volcanii* Pilin N-Glycans with Diverse Roles in Pilus Biosynthesis, Adhesion, and
440 Microcolony Formation. *J Biol Chem* 291:10602–10614.

441 24. Holten MP, Fonseca DR, Costa KC. 2021. The Oligosaccharyltransferase AglB Supports
442 Surface-Associated Growth and Iron Oxidation in *Methanococcus maripaludis*. *Appl*
443 *Environ Microbiol* 87.

444 25. Jarrell KF, Stark M, Nair DB, Chong JPJ. 2011. Flagella and pili are both necessary for
445 efficient attachment of *Methanococcus maripaludis* to surfaces: Flagella and pili necessary
446 for *M. maripaludis* attachment. *FEMS Microbiol Lett* 319:44–50.

447 26. Haiko J, Westerlund-Wikström B. 2013. The Role of the Bacterial Flagellum in Adhesion
448 and Virulence. *Biology* 2:1242–1267.

449 27. Belas R. 2014. Biofilms, flagella, and mechanosensing of surfaces by bacteria. *Trends*
450 *Microbiol* 22:517–527.

451 28. Flemming H-C, Wuertz S. 2019. Bacteria and archaea on Earth and their abundance in
452 biofilms. *Nat Rev Microbiol* 17:247–260.

453

454

455

456

457

458

459

460

461

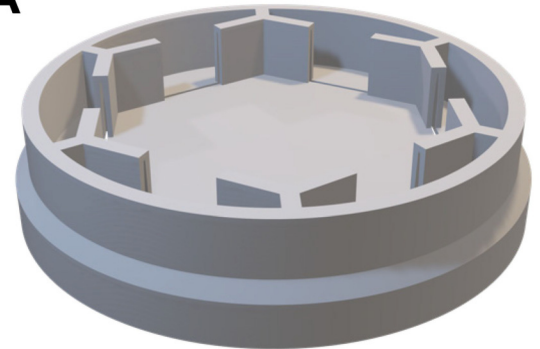
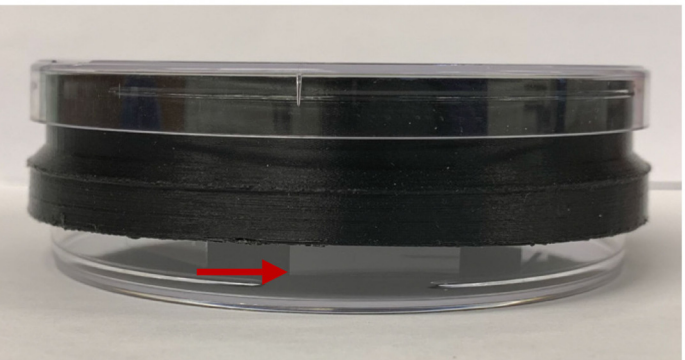
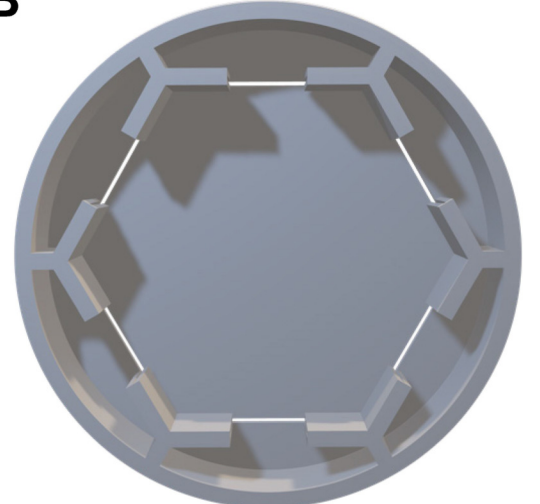
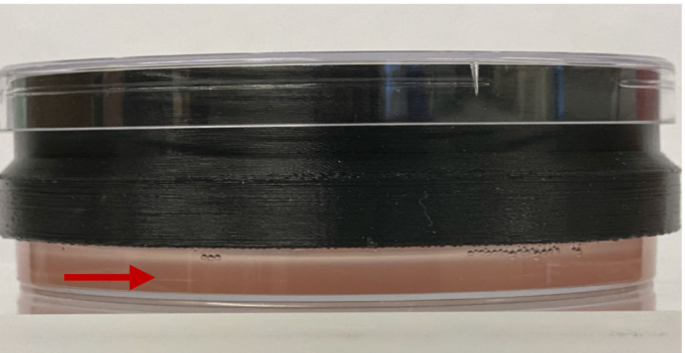
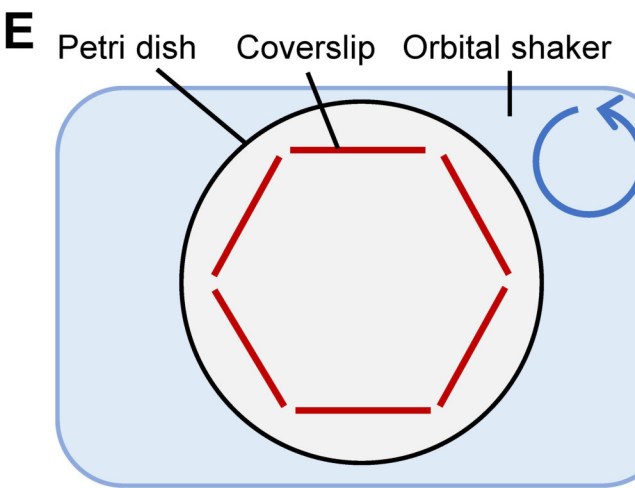
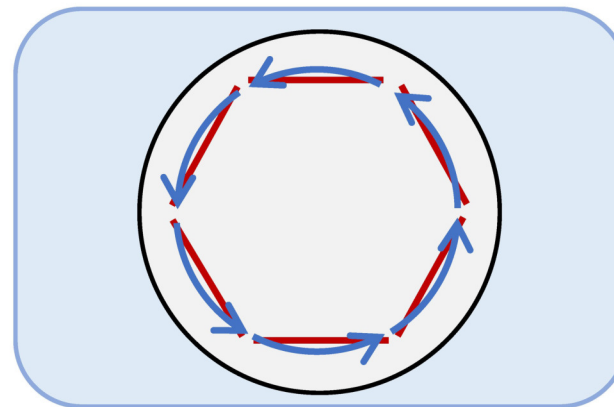
462 **Supplemental Material**

463

464 **Supplemental Figure 1: 3D-printing of the mPAD mount allows for straightforward**
465 **changes to its design.**

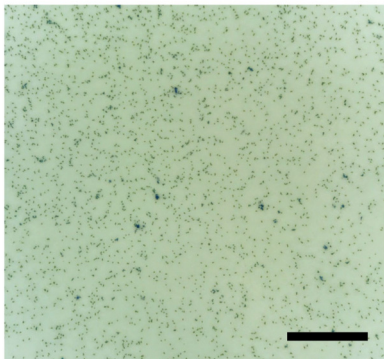
466

467

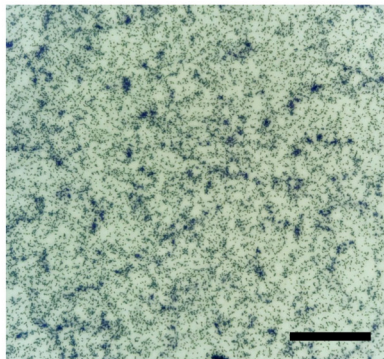
A**C****B****D****E****F**

Standing (12-well assay)

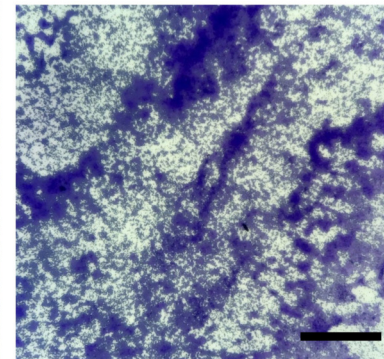
1 hour



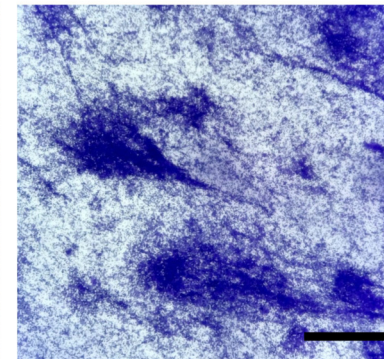
6 hours



20 hours



45 hours



PA14

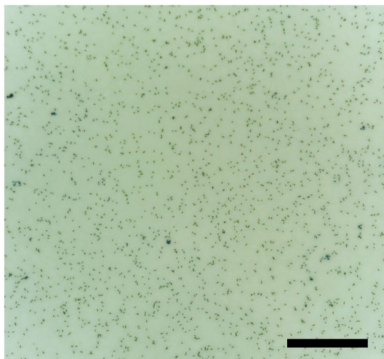
Δphz

Shaking (mPAD assay)

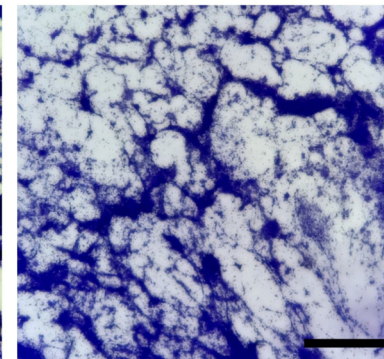
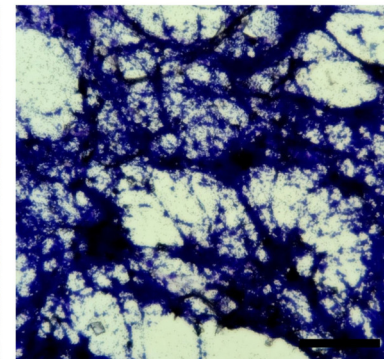
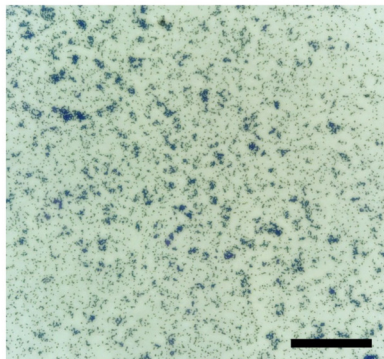
PA14

Δphz

1 hour

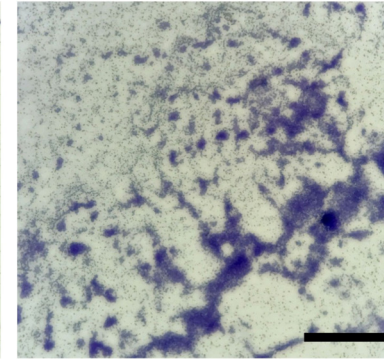
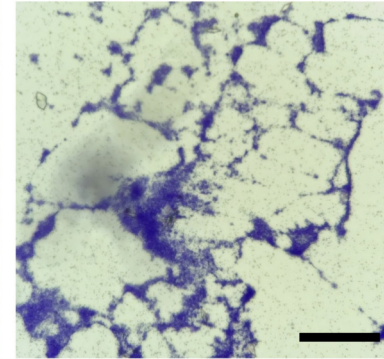
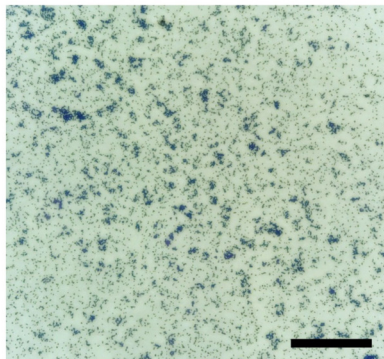


6 hours



20 hours

45 hours



Standing (12-well assay)

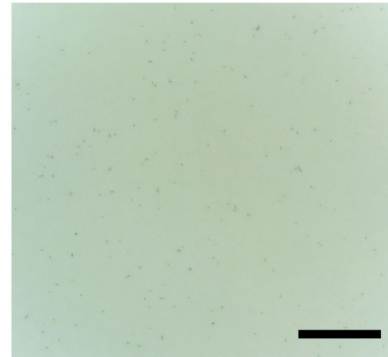
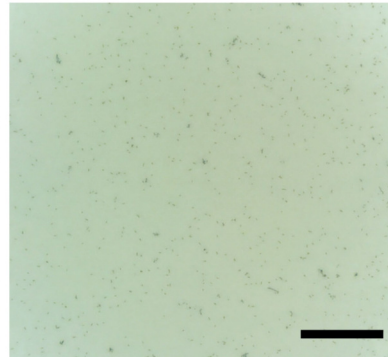
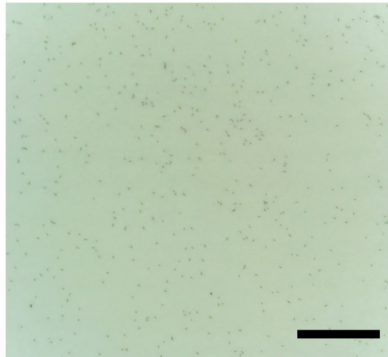
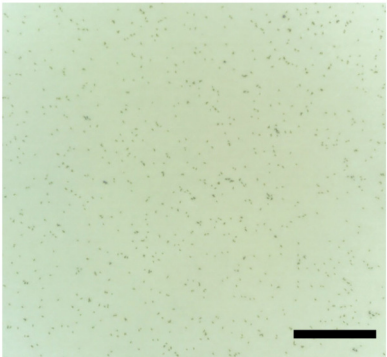
1 hour

6 hours

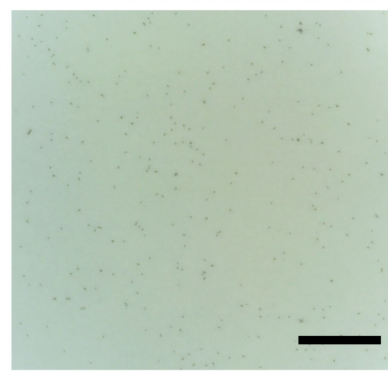
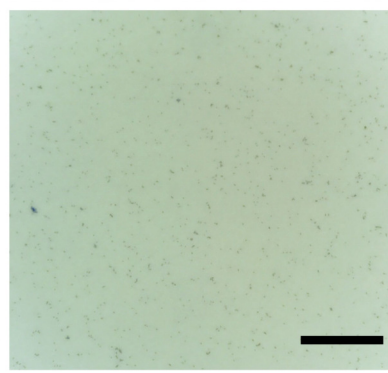
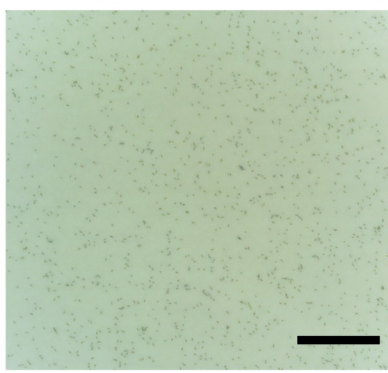
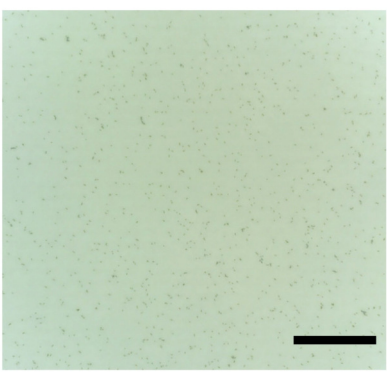
20 hours

45 hours

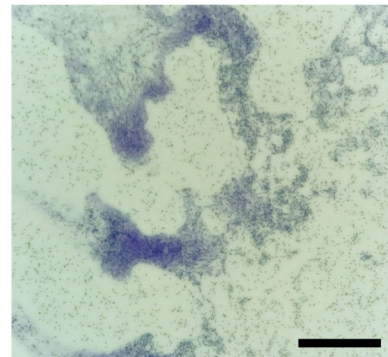
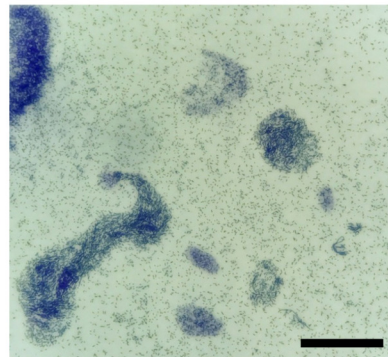
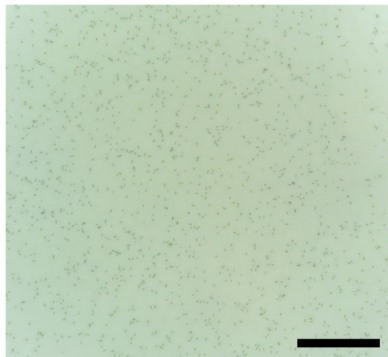
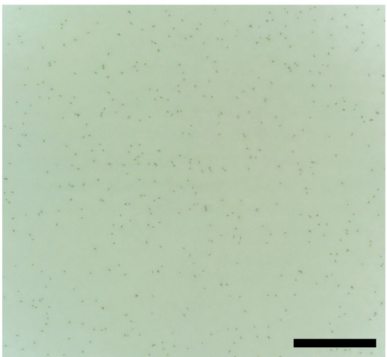
PA14



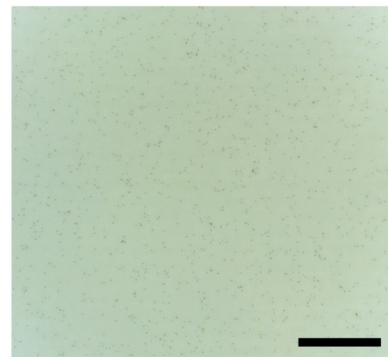
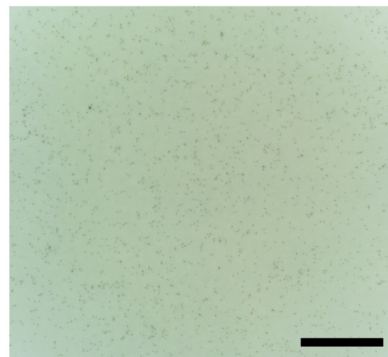
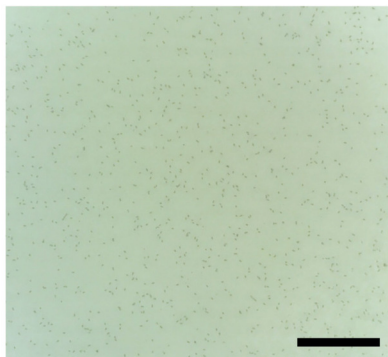
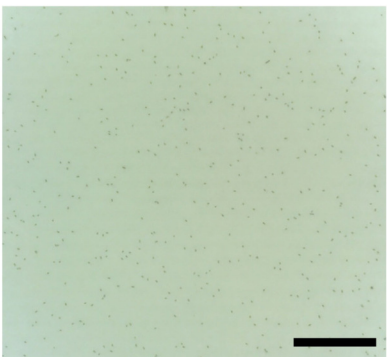
Δphz



PA14



Δphz

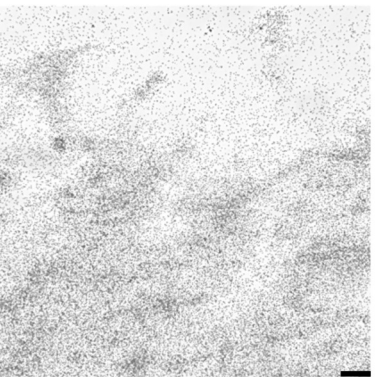
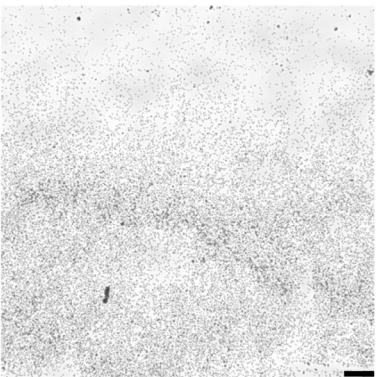
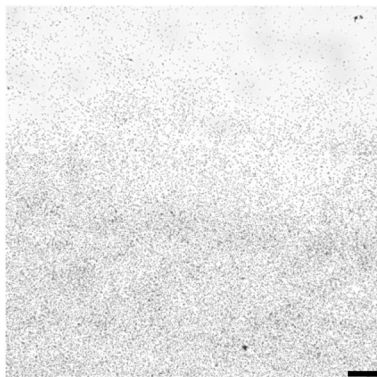


Standing (12-well assay)

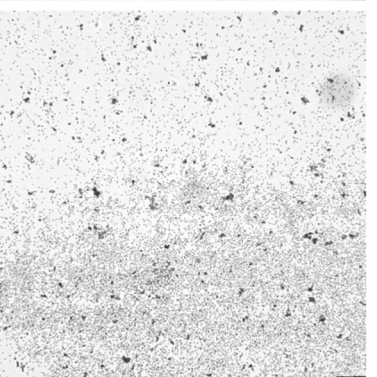
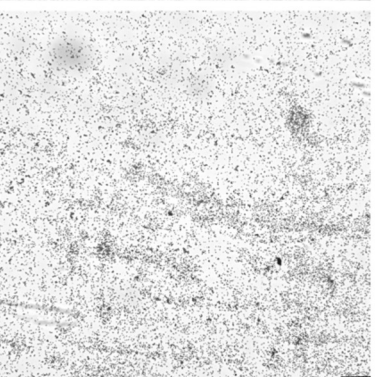
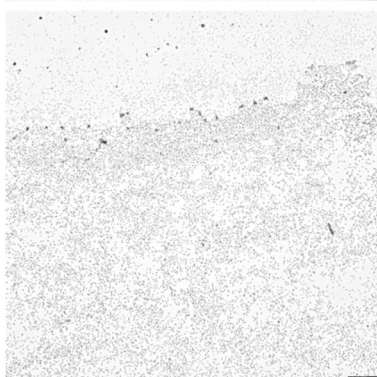
24 hours

120 hours

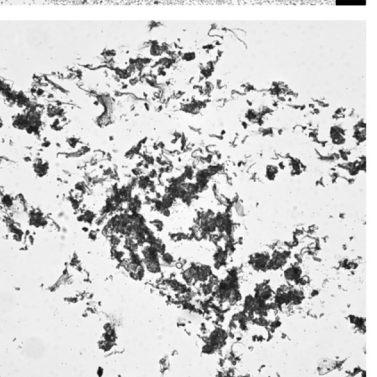
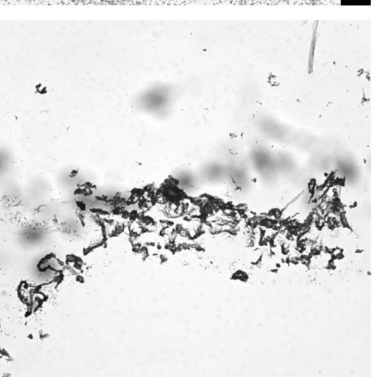
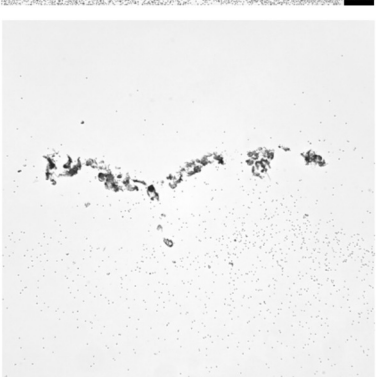
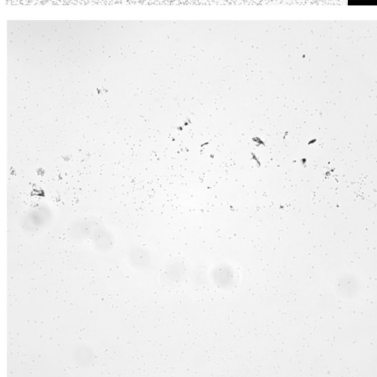
H53



$\Delta arlA1/2$



H53



Shaking (mPAD assay)

$\Delta arlA1/2$

